Secondary crystallization in $(Fe_{65}Co_{35})_{79.5+x}B_{13}Nb_{4-x}Si_2Cu_{1.5}$ and $(Fe_{65}Co_{35})_{83}B_{10}Nb_4Si_2Cu_1$ nanocomposite alloys

Samuel J. Kernion,[1,a)] Vladimir Keylin,[2] Joe Huth,[2] and Michael E. McHenry[1]
[1]*Materials Science and Engineering Department, Carnegie Mellon University, Pittsburgh, Pennsylvania 15213, USA*
[2]*Magnetics Technology Center, Division of Spang & Company, Pittsburgh, Pennsylvania 15238, USA*

(Presented 1 November 2011; received 23 September 2011; accepted 17 November 2011; published online 16 February 2012)

Here, secondary crystallization kinetics of high induction, low loss HTX002-type nanocomposite alloys with the compositions $(Fe_{65}Co_{35})_{79.5+x}B_{13}Nb_{4-x}Si_2Cu_{1.5}$ (x = 0-4) and $(Fe_{65}Co_{35})_{83}B_{10}Nb_4Si_2Cu_1$ are reported. The magnetization of the alloys was measured through the thermal cycle of 50 °C-700 °C-300 °C-800 °C-300 °C-900 °C-200 °C by vibrating sample magnetometry. In $(Fe_{65}Co_{35})_{79.5+x}B_{13}Nb_{4-x}Si_2Cu_{1.5}$ alloys, the stability of the $(Fe,Co,Nb)_{23}B_6$ (23-6) phase is increased with increasing Nb content. In the x = 4 alloy, $(Fe,Nb)_2B$ is the only secondary crystalline phase to form, demonstrating that Nb is necessary for the 23-6 phase to form. The $(Fe_{65}Co_{35})_{83}B_{10}Nb_4Si_2Cu_1$ alloy forms the 23-6 phase more readily than the x = 0 alloy, likely due to the lower B content. The kinetics of secondary crystallization are important to assess long-term ageing effects on the metastable microstructure at elevated temperatures. © *2012 American Institute of Physics*. [doi:10.1063/1.3677830]

I. INTRODUCTION

Nanocomposite alloys (HTX002-type[1–3]) of composition $(Fe_{65}Co_{35})_{79.5+x}B_{13}Nb_{4-x}Si_2Cu_{1.5}$ (x = 0-4) and $(Fe_{65}Co_{35})_{83}B_{10}Nb_4Si_2Cu_1$, designated alloy "10-4", were studied to determine the kinetics of and phase evolution in secondary crystallization. HTX002 nanocomposites exhibit high saturation flux densities up to 1.85 T and low losses at kHz level frequencies,[1–3] making them promising for inductive components in high frequency power electronic applications. The formation of crystalline phases other than α-FeCo deteriorate these properties. Therefore, understanding the kinetics of the secondary transformation and stability of the phases that form at high temperatures is useful in designing nanocomposites with stable microstructures. Two boride phases typically can form in nanocomposites with Nb and B as glass formers, $(Fe,Co,Nb)_{23}B_6$ and $(Fe,Co,Nb)_2B$.[4–8] These are referred to in the following discussion as the 23-6 and 2-1 phase, regardless of the transition metal content.

The cubic 23-6 phase is based on the $Cr_{23}C_6$ prototype structure with the *Fm-3m* space group (Fig. 1(a)). The tetragonal 2-1 phase has the Al_2Cu prototype structure and *I4/mcm* space group (Fig. 1(b)). In nanocomposites having Fe as the only late transition metal, Fe_2B is the most stable boride phase.[4] Experiment and theoretical calculations show that substitution of Co for Fe stabilizes the 23-6 phase.[5–7] Moreover, 3D atom probe studies of a Nb-containing nanocomposite showed that the 23-6 phase contains 7.5 at. % Nb, which corresponds well with that required to fill the spacious 8c sites in the 23-6 unit cell.[8] It is well-known that Nb inhibits the formation of the 2-1 phase, which explains an increase in the secondary crystallization temperature with increasing Nb-content.[2,3] In this work, the effect of the non-magnetic species Nb and B on phase selection is explored.

II. EXPERIMENTAL PROCEDURE

Ingots with nominal compositions $(Fe_{65}Co_{35})_{83}B_{10}Nb_4Si_2Cu_1$ and $(Fe_{65}Co_{35})_{79.5+x}B_{13}Nb_{4-x}Si_2Cu_{1.5}$ (x = 0-4) were synthesized from constituent elements by induction melting. A planar flow caster was used to cast 2-3 kg of each ingot into ribbon. As-cast ribbon was cut into 3 mm radius discs. A stack of 10–15 discs of each composition were taken through a heating and cooling cycle of 50 °C–700 °C–300 °C–800 °C–300 °C–900 °C–200 °C at 5 °C/min, while their magnetic moment was measured under an applied field of 2.5 kOe by a Lake Shore 7407 vibrating sample magnetometer (VSM). The samples were allowed to dwell for 1800 s at the end of each heating run to ensure thermal equilibrium. The presence of phases was confirmed by annealing as-cast ribbon at 900 °C for 1800 s followed by scanning on an x-ray diffractometer (XRD) ($\lambda = 0.154$ nm).

III. RESULTS AND DISCUSSION

Magnetization as a function of temperature for the $(Fe_{65}Co_{35})_{79.5+x}B_{13}Nb_{4-x}Si_2Cu_{1.5}$ alloys is shown in Fig. 2. The omitted cooling curves do not provide unique information compared to their subsequent heating curves. Data for all plots were normalized to the magnetic moment of the as-cast material at 50 °C. The first observed increase in magnetization on heating (Fig. 2(a)) is caused by repartitioning of the magnetic species in α-FeCo nucleation and growth. The onset temperature of this primary crystallization increases with Nb content. The magnetization then decreases as the magnetic moment of the residual amorphous phase approaches its Curie temperature (T_c).

a)Author to whom correspondence should be addressed. Electronic mail: skernion@andrew.cmu.edu.

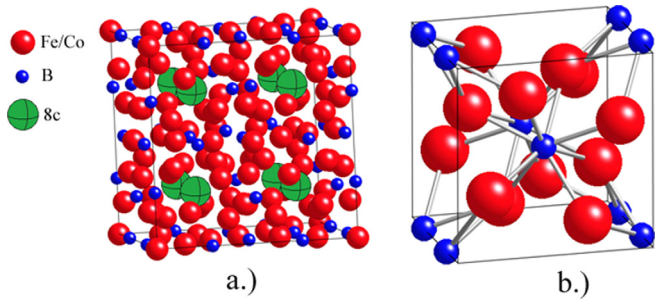

FIG. 1. (Color online) Models of (a) 23-6 phase showing B atoms, Fe or Co atoms, and the 8c special positions that Nb can potentially fill and (b) 2-1 phase with B atoms and Fe/Co/Nb atoms.

The further abrupt increase in magnetization observed in Fig. 2(a) for the x = 4-2 alloys is due to secondary crystallization of the residual amorphous matrix into the magnetic 2-1 phase. The 2-1 phase is identified based on its T_c, which is noted at 670 °C by the drop in magnetization.[9] The alloys with x = 1 and 0 display continued growth of the primary phase after the amorphous phase T_c. There is no magnetization burst at secondary crystallization temperatures of these alloys, but instead a drop off occurs. This does not give indicate which secondary phase forms, as both the 2-1 and 23-6 phases are non-magnetic at these temperatures. The decrease in magnetization does imply that α-FeCo is partially transformed to a non-magnetic phase.

The curves on heating from 300-800 °C (Fig. 2(b)) show that the 2-1 phase was the prevalent secondary phase to form in alloys with x = 4-1 after the first heating run, as a Curie tail is evident around 700 °C. The x = 4 alloy displays a higher T_c of the 2-1 phase, likely due to the reduced Nb content. The x = 0 alloy shows two Curie transitions as the temperature is increased, indicated by the two vertical lines. The first, seen at 550°, is attributed to the 23-6 phase,[6] while the second at 700 °C is from the 2-1 phase. This coexistence is explained by the stabilization of the 23-6 phase by enrichment of the residual matrix in Co and Nb.

During primary crystallization, the amorphous matrix is enriched in glass formers. We have also shown that the growing bcc α-FeCo crystallites tend to have an Fe:Co ratio of 70:30, which is higher than the bulk ratio.[10] This partitioning leaves the amorphous matrix with a higher concentration of Co compared to the nominal Fe:Co ratio. This indicates faster Fe diffusion as compared to Co diffusion through the Nb that builds up as a shell on the growing crystallite. Fe is known to have higher mobility than Co in FeCo-based alloys.[11] The Nb shell thickness depends on the Nb concentration, so the rate of Fe diffusion through the shell will be slower for alloys with a high Nb content. This delays the enrichment of the amorphous phase in Co and B and leads to higher secondary transformation temperatures.

The fact that the residual amorphous matrix is not only enriched in glass formers but also in Co as the crystallites continue to grow lowers the free energy of the 23-6 phase. In alloys with insufficient Nb content, the 2-1 phase nucleates before the composition becomes favorable for 23-6 phase formation. In the x = 0 alloy, there is enough Nb to inhibit formation of the 2-1 phase until a composition and temperature

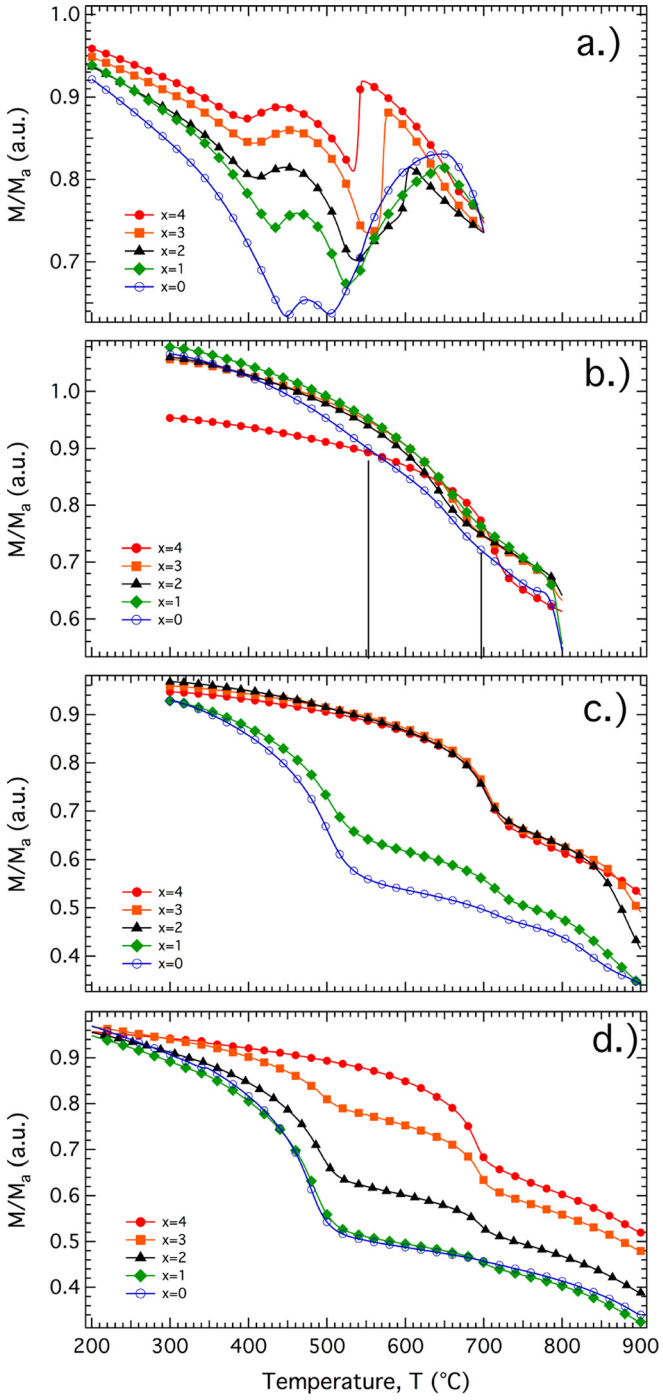

FIG. 2. (Color online) Normalized magnetization as a function of temperature for $(Fe_{65}Co_{35})_{79.5+x}B_{13}Nb_{4-x}Si_2Cu_{1.5}$ alloys on heating from (a) 200-700 °C, (b) 300-800 °C, and (c) 300-900 °C and on cooling from (d) 900-200 °C.

is reached where nucleation and growth of the 23-6 phase occurs. The 23-6 phase prefers Co over Fe and can readily incorporate Nb into the 8c sites, leaving the remaining amorphous matrix less enriched in those elements. It is proposed that the x = 0 alloys sits at such a composition that the removal of the Nb and Co from the residual amorphous matrix into the 23-6 phase stabilizes the 2-1 phase, resulting in their coexistence after heating to 700 °C.

This is reinforced by the subsequent heating from 300-900 °C (Fig. 2(c)), which shows that the dominant secondary

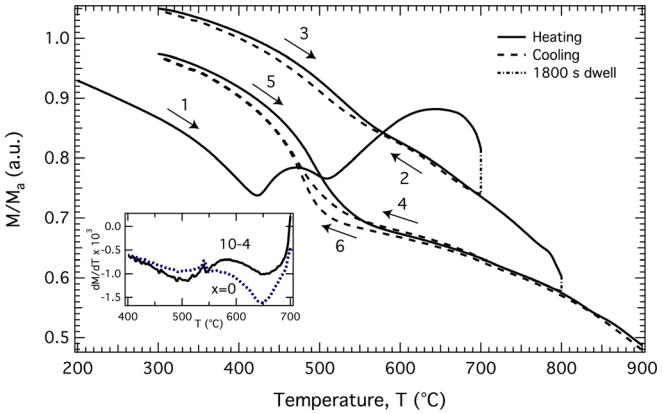

FIG. 3. (Color online) Magnetization as a function of temperature for the 10-4 alloy following the temperature profile of (1) heating to 700 °C, (2) cooling to 300 °C, (3) heating to 800 °C, (4) cooling to 300 °C, (5) heating to 900 °C, and (6) cooling to 300 °C.

phase of the x = 0 and x = 1 alloys after heating to 800 °C is the 23-6 phase, based on the large magnetic transition at 540 °C. The alloys with x = 2-4 still only show the 2-1 T_c. However, at the end, further phase transformation takes place, as indicated by the divergence of the x = 3 and 2 alloys from the x = 4 alloy. On cooling (Fig. 2(d)), this transformation is revealed to be the formation of the 23-6 phase, which is now present in the x = 3 and x = 2 alloys. The only alloy without an indication of 23-6 phase formation is the x = 4 alloy, demonstrating that Nb is necessary for 23-6 phase formation in this alloy system. Conversely, the 2-1 phase transition has entirely disappeared in the x = 0 alloy. This implies the 23-6 phase is more stable than the 2-1 phase, as long as there is Nb to incorporate.

Figure 3 shows the magnetization of the 10-4 alloy as a function of temperature over the same heating cycle. The magnetization follows a similar trend as the x = 0 alloy. In order to compare these alloys, the first derivative of the magnetization on cooling from 700-300 °C was calculated by the central differences method and is plotted in the inset of Fig. 3. The slope of the increase in moment from the magnetization of the 2-1 phase is greater in magnitude for the x = 0 alloy, while the increase from the 23-6 phase is greater in the 10-4 alloy. The magnetization of each phase at these temperatures would need to be known to quantitatively compare the volume fraction of each phase present, although it is clear that the ratio of 23-6 phase volume fraction to 2-1 phase volume fraction is higher in the 10-4 alloy. The 23-6 phase contains less B than the 2-1 phase, and it follows that the alloy with the lower B content would contain a higher volume fraction of the 23-6 phase.

The heating of stage (5) does not show any discernable transformation; however, on cooling in stage (6), the T_c of the 23-6 phase appears to have dropped. Research by Blázquez *et al.*[6] has shown that the T_c of the 23-6 phase decreases with Co-content. Co also acts to stabilize the 23-6 phase, so it is believed that further high temperature annealing allowed continued substitution of Co for Fe in the 23-6 phase. The identification of crystallization products is the first step in elucidating their role in determining the long-term stability of metastable nanocomposite microstructures. Future studies of secondary nanocrystallization kinetics will serve to suggest the limitations posed by secondary crystallization on the long-term stability of the nanocomposite microstructure with reduced glass former concentrations.[12] This is a more challenging problem in the process of secondary crystallization, because the products are often non-magnetic at the transformation temperatures and, therefore, kinetic magnetization studies[13–15] useful in studying primary crystallization are not relevant for these secondary crystallization events.

IV. CONCLUSIONS

High temperature magnetometry was used to show preferential boride-phase formation in FeCo-based nanocomposite materials. As Nb is removed from the $(FeCo)_{79.5+x}B_{13}Nb_{4-x}Si_2Cu_{1.5}$ composition, the 2-1 phase becomes increasingly stable. The alloy with 4 at. % Nb demonstrates a less definitive transformation, with both the 2-1 and 23-6 phases forming in the initial heating of the material. After heating to 900 °C, the 23-6 phase can be found in all the alloys with the exception of x = 4, implying it is thermodynamically stable in all alloys with Nb. Reduction of B-content from 13 at. % to 10 at. % also helps to stabilize the 23-6 phase. These results suggest there are different crystallization paths, depending on the growth inhibitor concentration.

ACKNOWLEDGMENTS

S.J.K. and M.E.M. acknowledge support from the ARL through Grant No. W911NF-08-2-0024.

[1]J. Long, M. E. McHenry, D. Urciuoli, V. Keylin, J. Huth, and T. Salem, J. Appl. Phys. **103**, 07E705 (2008).
[2]K. J. Miller, A. Wise, A. Leary, D. E. Laughlin, M. E. McHenry, V. Keylin, and J. Huth, J. Appl. Phys. **107**, 09A316 (2010).
[3]S. J. Kernion, K. J. Miller, S. Shen, V. Keylin, J. Huth, and M. E. McHenry, IEEE Trans Magn. **47**, 3452 (2011).
[4]M. Imafuku, S. Sato, H. Koshiba, E. Matsubara, and A. Inoue, Scr. Mater. **44**, 2369 (2001).
[5]P. R. Ohodnicki, Jr., N. C. Cates, D. E. Laughlin, M. E. McHenry, and M. Widom, Phys. Rev. B **78**, 144414 (2008).
[6]J. S. Blázquez, S. Lozano-Pérez, and A. Conde, Philos. Mag. Lett. **82**, 409 (2002).
[7]A. Hirata, Y. Hirotsu, K. Amiya, N. Nishiyama, and A. Inoue, Phys. Rev. B **80**, 140201 (2009).
[8]J. Long, P. R. Ohodnicki, D. E. Laughlin, M. E. McHenry, T. Ohkubo, and K. Hono, J. Appl. Phys. **101**, 09N114 (2007).
[9]L. Tukacs, M. C. Cadedle, and I. Vincze, J. Phys. F: Met. Phys. **5**, 800 (1975).
[10]D. H. Ping, Y. Q. Wu, K. Hono, M. A. Willard, M. E. McHenry, and D. E. Laughlin, Scr. Mater. **45**, 781 (2001).
[11]N. J. Jones, K. L. McNerny, A. T. Wise, M. Sorescu, M. E. McHenry, and D. E. Laughlin, J. Appl. Phys. **107**, 09A304 (2010).
[12]M. E. McHenry, F. Johnson, H. Okumura, T. Ohkubo, A. Hsiao, V. R. V. Ramanan, and D. E. Laughlin, Scr. Mater. **48**, 881 (2003).
[13]A. Hsiao, M. E. McHenry, M. Tamoria, and V. G. Harris, IEEE Trans. Magn. **37**, 2236 (2001).
[14]M. Tamoria, E. E. Carpenter, M. M. Miller, J. H. Claassen, B. N. Das, R. M. Stroud, L. K. Kurihara, R. K. Everett, M. A. Willard, A. Hsiao, M. E. McHenry, and V. G. Harris, IEEE Trans. Magn. **37**, 2264 (2001).
[15]A. Hsiao, M. E. McHenry, D. E. Laughlin, M. J. Kramer, C. Ashe, and T. Okubo, IEEE Trans. Magn. **38**, 2946 (2002).